

Interfacial assembly

NJUT

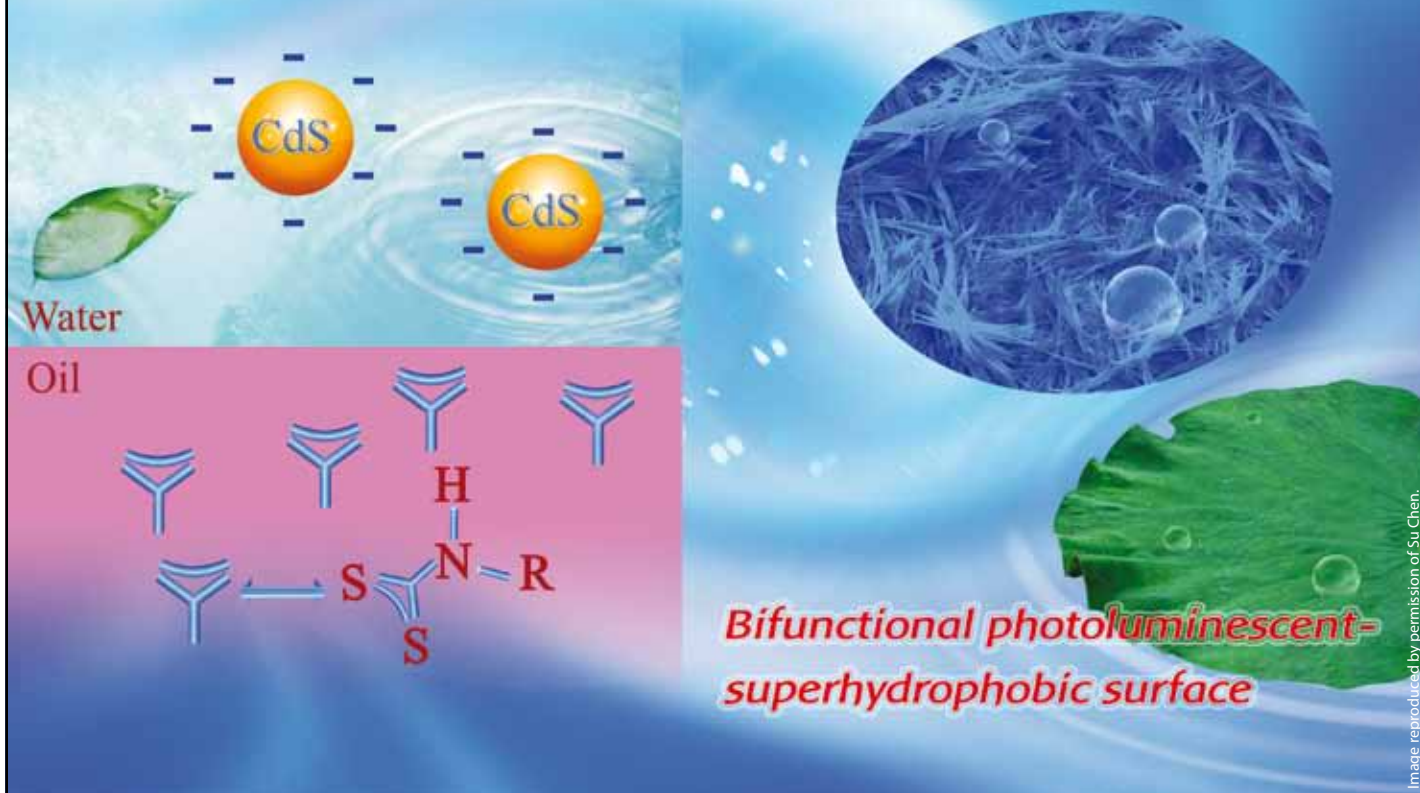


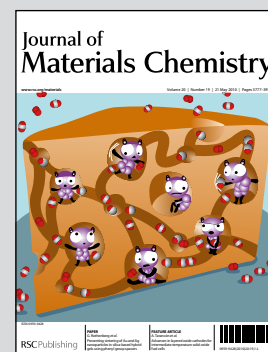
Image reproduced by permission of Su Chen.

Showcasing research efforts from Professor Su Chen's group at State Key Laboratory of Material-Oriented Chemical Engineering, Nanjing University of Technology, Nanjing, P. R. of China.

Title: Multiple-structured nanocrystals towards bifunctional photoluminescent-superhydrophobic surfaces

The fabrication of bifunctional photoluminescent-superhydrophobic surfaces can be induced by facile interfacial self-assembly of nanocrystals and dithiocarbamates, generating new strategies for diverse hierarchical structures of nanocrystals, e.g., wire-like, belt-like, and sheet-like microstructures. This approach serves as a new and efficient procedure for designing more practical photoluminescent-superhydrophobic films.

As featured in:



See Linrui Hou, Caifeng Wang, Li Chen and Su Chen, *J. Mater. Chem.*, 2010, **20**, 3863

RSC Publishing

www.rsc.org/materials

Registered Charity Number 207890

Multiple-structured nanocrystals towards bifunctional photoluminescent-superhydrophobic surfaces†

Linrui Hou, Caifeng Wang, Li Chen and Su Chen*

Received 21st December 2009, Accepted 16th February 2010

First published as an Advance Article on the web 15th March 2010

DOI: 10.1039/b926761a

We report a simple and efficient strategy for the preparation of diverse hierarchical structures of dithiocarbamate-functionalized CdS nanocrystals (NCs) exhibiting both photoluminescent and hydrophobic properties *via* a facile interfacial self-assembly technique. The ligand exchange reaction of thioglycolic acid (TGA) with dithiocarbamates at the biphasic interface endowed CdS with diversiform morphologies. Simultaneously, the resulting dithiocarbamate-functionalized NCs after interfacial self-assembly exhibit good photochemical stability and enhanced photoluminescence (PL) in comparison with the parent NCs. Moreover, the introduction of dithiocarbamate ligands with long alkyl chains can significantly enhance the hydrophobic properties of NCs in this case. By simply varying the directing ligands with different intrinsic hydrophobic natures, superhydrophobic surfaces constructed from the fluorescent NCs can be fabricated.

Introduction

Self-assembly architectures of nanocrystals (NCs) have attracted great attention because of their extensive scientific and industrial interest in areas such as light-emitting devices (LEDs),¹ nonlinear optical devices,² and nanosensors.³ To gain the desirable properties of NCs, tremendous efforts have been devoted to the development of photostability and compatibility of NCs.⁴ Among them, the surface chemical processing and organization of NCs are of major importance,⁵ because functional organic surface ligands can serve to heal NC surface defects, and allow NCs to organize into ordered hierarchical structures for the coupling of their size- and shape-dependent properties.^{6,7} Also, these organic surface ligands provide inorganic NCs with compatibility, stability and processability in a range of organic materials through favorable interactions. Recently, the water/oil interface has been widely used as an ideal platform for manipulating the self-assembly of NCs into hierarchical structures.^{8–10} Such an interface can favor prolonging the assembly time of NCs, thus healing defects and diversifying the structural complexity of NCs. Although great efforts on the interfacial assembly technique have been made for this purpose, the construction of versatile multiscale structures of NCs with desired properties still remains a challenge.

Recently, one of the important applications of these NCs is their use as fluorescent films. A fluorescent film possesses more favorable properties than a molecular fluorescent solution and it

can easily be made into devices, along with being reusable.¹¹ However, the commonly used organic materials have short lifetimes which require the films to be changed frequently. Films made of inorganic fluorescent materials will have a longer stability period, but they unfortunately are still sparsely reported for this purpose. Therefore, the fabrication of fluorescent and self-cleaning superhydrophobic films will be of great promise for smart materials with optical properties. Specifically, hierarchical structures constructed on the micro/nanoscale give an efficient approach to achieve superhydrophobic surfaces, which are defined as those with a water contact angle (CA) larger than 150 °C.^{12–14} Char and co-workers have prepared smart superhydrophobic films exhibiting responsive optical properties, where hydrophobic fluorophores were incorporated into the hydrophobic polystyrene (PS) cores of charged block copolymer micelles by self-diffusion.¹⁵ Although a little progress has been achieved,^{15,16} there are limited reports on the fabrication of bifunctional photoluminescent-superhydrophobic films.

So far, thiols are the most common motifs which present the strongest affinity for NCs but they suffer from a major drawback, instability toward photooxidation, thus limiting the practical applications of these NCs.^{17–19} To improve the resistance of NCs against photooxidation, introduction of dithiocarbamate moieties for fabrication of NCs may be an efficient method due to their strong chelating capability to metal atoms.^{20–23} In this work, we report a simple and efficient strategy for the preparation of diverse hierarchical structures of dithiocarbamate-functionalized CdS NCs exhibiting both photoluminescent and hydrophobic properties in a facile interfacial self-assembly process. The ligand exchange reaction of thioglycolic acid (TGA) with dithiocarbamates at the biphasic interface afforded hierarchical structures with diversiform morphologies. The resulting dithiocarbamate-functionalized NCs offer advantages: good stability toward photooxidation, enhanced PL, and controlled hierarchical structure. Moreover, this procedure opens a way to fabricate superhydrophobic surfaces of NCs by simply varying

State Key Laboratory of Material-Oriented Chemical Engineering, College of Chemistry and Chemical Engineering, Nanjing University of Technology, Nanjing, 210009 Xin Mofan Rd. 5#, P. R. of China. E-mail: chensu@njut.edu.cn; Fax: +86-25-83587194; Tel: +86-25-83587194

† Electronic supplementary information (ESI) available: Summaries of the various characterization studies, including the phase transfer experiment and the results of X-ray diffraction (XRD), FT-IR, ¹H NMR, and contact angle (CA) measurements. See DOI: 10.1039/b926761a

the directing ligands with different intrinsic hydrophobic nature. Also, it represents the first example of hierarchical surfaces created by small organic ligand functionalized NCs exhibiting simultaneous luminescence and superhydrophobicity.

Experimental

Materials

Cadmium chloride ($\text{CdCl}_2 \cdot 2.5\text{H}_2\text{O}$), thioglycolic acid (TGA), sodium sulfide ($\text{Na}_2\text{S} \cdot 9\text{H}_2\text{O}$), sodium hydroxide (NaOH), propylamine (PAm), octylamine (OAm), dodecylamine (DDAm), cyclohexylamine (CHAm), aniline (An), propylene acrylamide (PAAm), carbon disulfide (CS_2) and chloroform (CHCl_3) were of analytical grade and used as received.

Synthesis of water-soluble CdS NCs

The TGA-stabilized CdS NCs were synthesized according to a modified literature method.¹⁹ Typically, TGA (0.46 g, 5 mmol) dissolved in deionized water (10 mL) was added to a solution of $\text{CdCl}_2 \cdot 2.5\text{H}_2\text{O}$ (0.571 g, 2.5 mmol) in deionized water (20 mL) under vigorous stirring, followed by adjusting the pH value to 7 by dropwise addition of NaOH solution (5 M). $\text{Na}_2\text{S} \cdot 9\text{H}_2\text{O}$ (0.36 g, 1.5 mmol) dissolved in deionized water (20 mL) was then added dropwise into the above mixed solution under stirring. The reaction was carried out for an additional 3 h at room temperature.

Synthesis of dithiocarbamate ligands

A series of dithiocarbamate ligands were prepared as depicted in Fig. 1 (step I). A certain amount (5 mmol) of PAm, OAm, DDAm, CHAm, An or PAAm was added into a vessel containing CHCl_3 (45 mL). Then CS_2 (5 mmol) dissolved in CHCl_3 (5 mL) was added dropwise. The resulting solutions were stirred for 3 h at room temperature and stored for use in the next step.

Synthesis of dithiocarbamate-functionalized CdS NCs

The dithiocarbamate-functionalized CdS NCs were prepared as depicted in Fig. 1 (step II). The aqueous solution of TGA-stabilized CdS NCs was layered carefully on top of the CHCl_3 solution containing dithiocarbamate ligand in a vessel, which was sealed and maintained at room temperature for several days, and the NCs were slowly transferred from the water into the oil phase *via* an interfacial diffusion process (ESI,† Fig. S1). Finally, the chloroform phase containing dithiocarbamate-functionalized CdS NCs was collected, precipitated by addition of ethanol, and then isolated by centrifugation.

Preparation of bifunctional photoluminescent-hydrophobic films

The glass slide was rinsed with water prior to use. The NC solution was directly spin-coated onto the glass until a film was formed, and the thickness was calculated to be *ca.* 0.3 mm. The applied coatings were kept at room temperature for a week to remove residual solvent.

Characterization

Ultraviolet–visible (UV-vis) spectra were recorded on a Perkin-Elmer Lambda 900 UV-vis spectrometer. The X-ray diffraction (XRD) patterns were conducted on a Bruker-AXS D8 ADVANCE X-ray diffractometer with $\text{Cu-K}\alpha$ radiation ($\lambda = 0.1542 \text{ nm}$) at a scanning speed of 60 rpm over 2θ range of $10\text{--}80^\circ$. Fluorescence spectra were recorded on a Varian Cary Eclipse spectrofluorometer with a 360 nm laser beam as a light source, and the quantum yield (QY) was calculated by comparing with 9,10-DPA with quantum yield at 95%. ^1H Nuclear Magnetic Resonance (NMR) spectra were obtained on a Bruker ADVANCE DPX 400 spectrometer and chemical shifts are given in ppm relative to CHCl_3 (7.26 ppm). Transmission electron microscope (TEM) images were collected on a JEOL JEM-2100 electron microscope. High-resolution transmission electron microscopic (HRTEM) observation and electron diffraction patterns were performed with a JEOL JEM-2010 transmission electron microscope. The microstructures of the dithiocarbamate-functionalized NCs were observed by scanning electron microscopy (SEM) with a QUANTA 200 (Philips-FEI, Holland) instrument at 30.0 kV. Fourier transform infrared (FT-IR) spectra were recorded on a Nicolet 6700 FT-IR spectrometer: the samples were ground with KBr crystals, and the mixture was pressed into a pellet for IR measurement with 32 scans from 4000 to 500 cm^{-1} at a resolution of 4 cm^{-1} . Contact angles (CAs) of a $5 \mu\text{L}$ water droplet on the surface were measured with a KRÜSS DSA100 (KRÜSS, Germany) contact angle system at ambient temperature. The mean value was calculated from at least five individual measurements.

Results and discussion

TGA-stabilized CdS NCs were synthesized by the reaction of cadmium chloride and sulfur ions in the presence of TGA as the organic ligand. The overall procedure for the self-assembly of NCs is illustrated in Fig. 1. Firstly, a series of dithiocarbamate ligands (D-PAm, D-OAm, D-DDAm, D-CHAm, D-An and D-PAAm) are prepared with the reaction of CS_2 and the

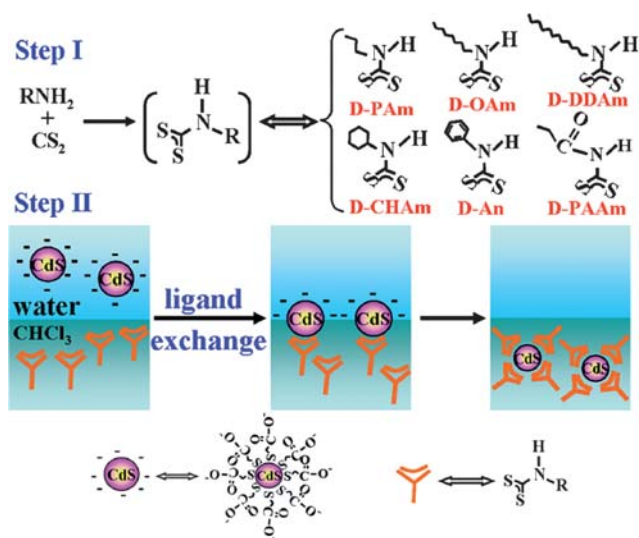


Fig. 1 Illustration of the route for the synthesis of the dithiocarbamate-functionalized CdS NCs.

corresponding amines in CHCl_3 (Fig. 1, step I). Subsequently, the resulting hydrophobic dithiocarbamates are used as exchange ligands to replace the original hydrophilic ligand TGA *via* the $\text{H}_2\text{O}-\text{CHCl}_3$ interface, where water-soluble TGA-stabilized CdS NCs are finally converted to oil-soluble dithiocarbamate-functionalized CdS NCs and a slow phase transfer of NCs from the aqueous phase into the chloroform phase occurs (Fig. 1, Step II). The digital pictures of the interfacial reactions as a function of reaction time further visually confirm that the CdS NCs are actually transferred slowly from the aqueous to the chloroform phase with the reaction time (ESI,† Fig. S1). These changes in FT-IR and ^1H NMR spectra before and after ligand exchange are indications of displacement of the original hydrophilic ligand TGA with the hydrophobic dithiocarbamate ligand (ESI,† Fig. S2–3).

The strategy involves the selection of suitable experimental conditions. Fig. 2a shows the PL spectra of D-DDAm-functionalized CdS NCs (CdS-D-DDAm) in chloroform phase after phase transfer under different molar ratios of CS_2 to amine (τ). The PL intensity of CdS-D-DDAm increases gradually with the increase of τ value and reaches a maximum at $\tau = 1/1$, while further increase of τ results in the decrease of the PL intensity. This behavior indicates that the formation of enough dithiocarbamates (*i.e.* stoichiometric ratio of CS_2 to amine) can guarantee the achievement of phase transfer and PL enhancement, whereas redundant CS_2 adsorbed on the surface of NCs can act as new trap centers to induce the decrease or even extinction of PL intensity. Fig. 2b presents the temporal evolution of PL spectra for CdS-D-DDAm during the phase transfer process. As the reaction time increases, the PL intensity of CdS-D-DDAm increases and reaches a maximum at 25 d, which can be attributed to the better surface passivation of NCs.²⁴ However, further prolongation of the reaction time results in the decrease of PL intensity due to the emerging of new surface traps in the end products.^{24,25} Based on the optimal experimental procedure with $\tau = 1/1$ and reaction time of 25 d, the interfacial assemblies of CdS NCs with various dithiocarbamates were carried out. The XRD pattern for the parent CdS NCs (ESI,† Fig. S4a) shows the face-centered cubic CdS phase and matches well with JCPDS card No. 21-0829, indicated by the blue vertical lines in ESI,† Fig. S4. The broadening of peaks originates from the small size of CdS NCs. By using the Debye–Scherrer equation,²⁶ the average crystallite size of CdS NCs is estimated to be 4.0 nm. In addition, the XRD patterns for these dithiocarbamate-functionalized CdS

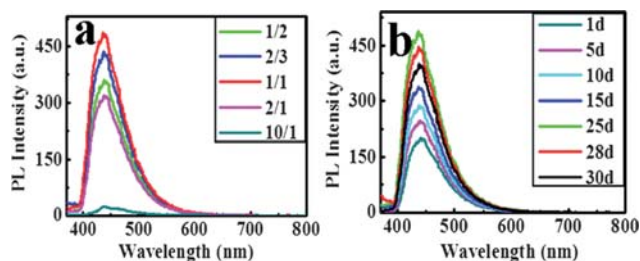


Fig. 2 (a) PL spectra of CdS-D-DDAm with different τ values ($\tau = 1/2$, $2/3$, $1/1$, $2/1$, and $10/1$, reaction time: 25 d, $\lambda_{\text{ex}} = 360$ nm). (b) Temporal evolution of PL spectra for CdS-D-DDAm during the phase transfer process ($\tau = 1/1$, $\lambda_{\text{ex}} = 360$ nm).

NCs (ESI,† Fig. S4b–g) are almost the same as that of the parent TGA-stabilized CdS NCs, which means that the surface ligand exchange reaction of dithiocarbamate with TGA does not change their parent crystal structure.

We explored the interfacial self-assembly behavior of TGA-stabilized NCs with dithiocarbamates bearing different alkyl side chains. The capping layer of CdS NCs was exchanged for dithiocarbamates with alkyl chains varying in length between 3 and 12 carbon atoms (C_3 for D-PAM, C_8 for D-OAm and C_{12} for D-DDAm, Fig. 1), and different self-assembly structures of NCs were obtained (Fig. 3a–c). D-PAM-functionalized CdS NCs (CdS-D-PAM) exhibit the structure of uniform braid-like microfringes consisting of nanowires with diameter of about 50 nm (inset in Fig. 3a). D-OAm-functionalized CdS NCs (CdS-D-OAm) show belt-like morphology with about 0.6 μm width, 80 nm thickness, and microscale length (inset in Fig. 3b). CdS-D-DDAm demonstrates a leaf-like microstructure with average length of 20 μm and width of 1 μm (Fig. 3c). The results indicate the length of the alkyl chain in the dithiocarbamate can serve to affect the morphologies of the end NC products during the interfacial self-assembly process.

For the different self-assembly morphologies of NCs, we tentatively investigated the effects of the length of the alkyl chain in the dithiocarbamate, and we attributed this structural variation to the combination of an oriented attachment mechanism (dipolar-dipolar interaction) and a diffusion mechanism.^{27–29} As shown in Fig. 4, dithiocarbamate ligand with strong chelation in the chloroform phase drags TGA-stabilized NCs from the aqueous phase to the biphasic interface where the ligand exchange reaction happens. When the short alkyl chain dithiocarbamate D-PAM is used as the exchange ligand, the NCs driven under dipolar-dipolar interaction rearrange orderly to obtain a wire-like structure. However, a longer alkyl chain results in a slower reaction rate and a longer assembly time due to the smaller diffusion coefficient.²⁹ Then, the misorientation of the constructing units occurs with the increase of length of the alkyl chain, thus leading to the gradual increasing of the dimension of the wire. Therefore, the self-assembly shapes of NCs vary from

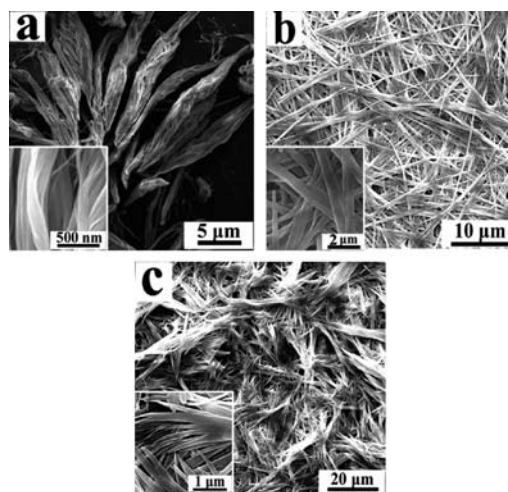


Fig. 3 SEM images of (a) CdS-D-PAM, (b) CdS-D-OAm, and (c) CdS-D-DDAm ($\tau = 1/1$, reaction time: 25 d).

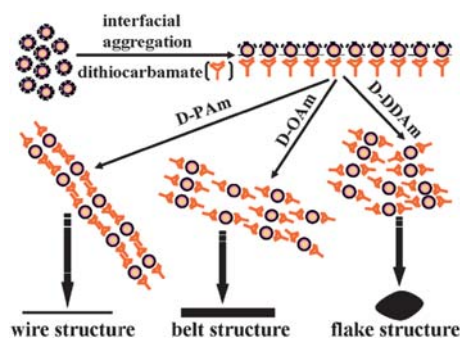


Fig. 4 Schematic representation of the interfacial assembly behaviors of TGA-stabilized NCs (●) with dithiocarbamates.

wire-like, belt-like, to flake-like structures with the increase of the alkyl chain length of the dithiocarbamates.

Perhaps more interestingly, the exchange of the surface capping ligand doesn't change the particle size of NCs, but significantly improves their luminescence. From the UV-vis absorption spectra (Fig. 5a), it can be found that the positions of the maximum absorption peaks of CdS-D-PAm, CdS-D-OAm and CdS-D-DDAm are almost unchanged in comparison with that of the parent TGA-CdS NCs, indicating the unchanged size of NCs during the interfacial assembly process. Fig. 5b shows the corresponding PL spectra and luminescent photographs of CdS NCs before and after ligand exchange reaction. The PL emission of TGA-stabilized CdS NCs is dominated by broad trap emission and yellow luminescence, while almost all dithiocarbamate-functionalized CdS NCs show narrow blue-shift exciton emission and improved PL intensity (except CdS-D-PAm). The difference in PL properties may be attributed to surface structural reconstruction of NCs *via* ligand exchange.³⁰ As documented in some reports, the ligand exchange on the surface of NCs led to the decrease or even quenching of luminescence,^{31,32} which also happened in the ligand exchange reaction of TOPO-stabilized CdSe NCs with dithiocarbamate carried out in a homogeneous system.²² However, in our work, the two-phase interfacial synthesis method may provide prolonged assembly (surface reconstruction) time and offer better passivation on NCs to heal surface defects, thus resulting in improved PL. The QYs of as-prepared NCs after the interfacial assembly are improved from 6.8% (TGA-CdS NCs) to 11.2% (CdS-D-PAm), 17.9%

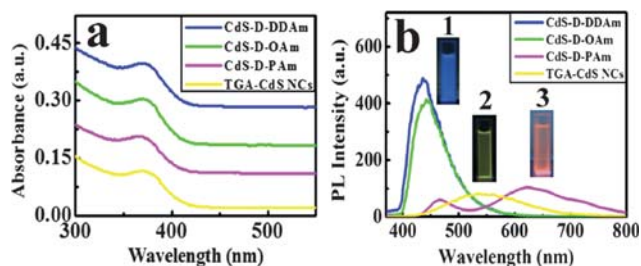


Fig. 5 UV-vis absorption (a) and PL (b) spectra of TGA-stabilized CdS NCs, CdS-D-PAm, CdS-D-OAm and CdS-D-DDAm ($\lambda_{\text{ex}} = 360$ nm). The insets of (b) are photographs of CHCl_3 solutions of (1) CdS-D-DDAm, (2) TGA-stabilized CdS NCs and (3) CdS-D-PAm taken under irradiation with a 302 nm UV light.

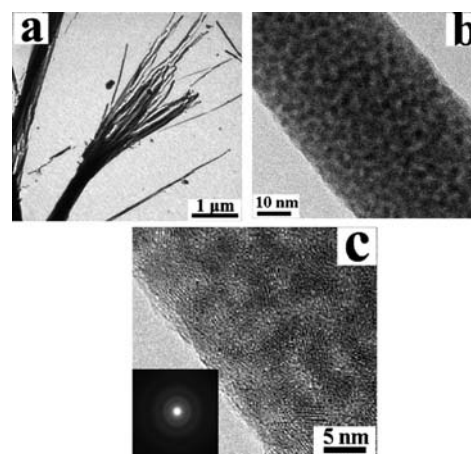


Fig. 6 TEM (a) and HRTEM (b, c) of CdS-D-PAm. Inset: corresponding SAED pattern.

(CdS-D-OAm) and 21.3% (CdS-D-DDAm). Another advantage of the as-prepared NCs herein is excellent photochemical stability: the quenching of luminescence of dithiocarbamate-functionalized NCs does not occur even after more than 6 months, while TGA-CdS NCs present a decreased PL after 6 months (ESI,† Fig. S5), which could be attributed to the strong chelation effects of dithiocarbamates to the metal atoms.^{20–22} This good PL stability makes the as-prepared self-assembled micro/nanostructure of NCs able to produce fluorescent films with high performance.

Evidence for the shape formation arising from the self-assembly of NCs can be directly confirmed from the HRTEM measurement. CdS-D-PAm was adopted as a model to investigate the interfacial self-assembly behavior of NCs. Fig. 6a–c show the self-assembly structures of CdS-D-PAm. As evident from Fig. 6a, the product is aggregated nanowires with diameters of about 50 nm. In the nanowires, the non-fused NCs retained the final CdS structure, demonstrating an excellent dispersion without obvious aggregation (Fig. 6b). The HRTEM image shown in Fig. 6c depicts the assembly of NCs with differently oriented lattice planes within the nanowire, and the clear lattice image indicates the certain crystallinity of NCs. The detectable rings in the selected area electron diffraction (SAED) pattern further indicate the small grain polycrystalline structure of NCs (inset in Fig. 6c).

The self-assembly architectures of NCs and their optical properties are affected not only by the length of the alkyl chain in dithiocarbamate as described above, but also by the use of other dithiocarbamates with pendant ring or amide groups. Typical SEM images of dithiocarbamate-functionalized CdS NCs of CdS-D-CHAm, CdS-D-An and CdS-D-PAAm are shown in Fig. 7a–c. CdS-D-CHAm is well-defined microsheets with unequal six sides having thickness of about 40 nm (Fig. 7a). CdS-D-An shows hackle-like nanobelt structure with width of about 200 nm, thickness of about 25 nm and microscale length (Fig. 7b). Additionally, CdS-D-PAAm has regular nanobelt structure with width of about 200 nm, thickness of about 60 nm and microscale length (Fig. 7c). The UV-vis measurements (Fig. 8a) show that the size of NCs almost remains unchanged during the interfacial assembly process. Simultaneously, the

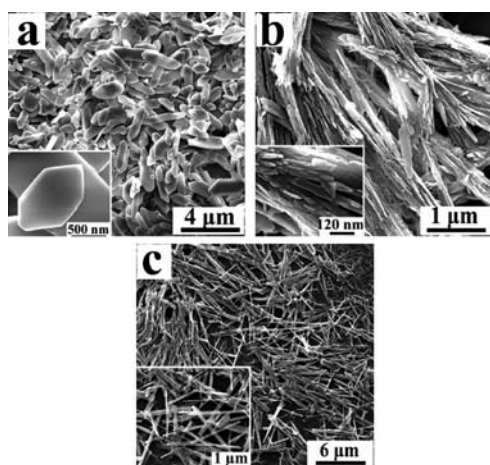


Fig. 7 SEM images of (a) CdS-D-CHAm, (b) CdS-D-An and (c) CdS-D-PAAm ($\tau = 1/1$, reaction time: 25 d).

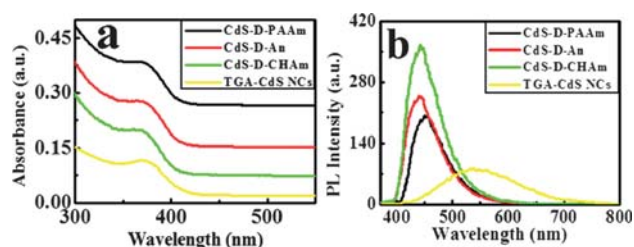


Fig. 8 UV-vis absorption (a) and PL (b) spectra of TGA-stabilized CdS NCs, CdS-D-CHAm, CdS-D-An and CdS-D-PAAm ($\lambda_{\text{ex}} = 360$ nm).

spectroscopic studies indicate that all three as-prepared NCs also show narrow blue-shift exciton emission with PL enhancement in comparison with that of the parent NCs after ligand exchange reaction (Fig. 8b), and the QYs of CdS-D-CHAm, CdS-D-An and CdS-D-PAAm are 15.8%, 10.8% and 8.7%, respectively. Moreover, the PL quantum yields of CdS-D-PAAm, CdS-D-OAm, CdS-D-DDAm and CdS-D-CHAm are higher than those of CdS-D-An and CdS-D-PAAm (Table 1), which are ascribed to their different transfer of electrons. Alkyl group acting as a donor for the nitrogen atom contributes to the stability of dithiocarbamate,^{33–35} while both phenyl and acyl groups acting as an acceptor induce the delocalization of electronic pairs of the nitrogen atom.³³ Therefore, the stabilization of dithiocarbamate-functionalized CdS NCs is increased to result in

Table 1 The QYs of the TGA-stabilized CdS NCs and a series of dithiocarbamate-functionalized CdS NCs ($\tau = 1/1$, reaction time: 25 d, $\lambda_{\text{ex}} = 360$ nm)

Materials	QY (%)
TGA-CdS NCs	6.8
CdS-D-PAAm	11.2
CdS-D-OAm	17.9
CdS-D-DDAm	21.3
CdS-D-CHAm	15.8
CdS-D-An	10.8
CdS-D-PAAm	8.7

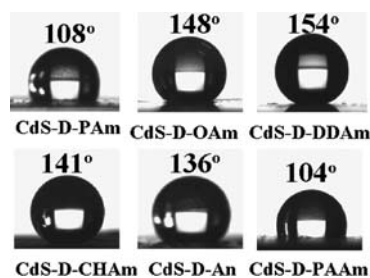


Fig. 9 Contact angles of the films of dithiocarbamate-functionalized CdS NCs.

PL enhancement when surface ligands with acceptor groups are substituted by those with donor groups.

Given that the self-assembled micro/nanostructure of NCs are constructed with the use of dithiocarbamates with hydrophobic nature and low surface energy, multifunctional films with tunable hydrophobicity and photoluminescence may be available. The solution of as-synthesized fluorescent dithiocarbamate-functionalized NCs was directly spin-coated onto glass to fabricate uniform NC films. The wettability of the films was evaluated by water CA measurements to be in the range 104–154° (Fig. 9), displaying their obvious hydrophobic properties in contrast with the film of TGA-stabilized CdS NCs (ESI,† Fig. S6). For the films governed by the chain dithiocarbamate-functionalized CdS NCs, the CA increases as the length of the alkyl side chains increases: the CA for the film treated with CdS-D-PAAm (C_3) is 108°, while the film created by CdS-D-DDAm (C_{12}) shows improved superhydrophobic properties with a CA up to 154°; this is due to dithiocarbamate with longer alkyl chain which has lower surface free energy. The results suggest that the structural variation of dithiocarbamates may provide an approach to control the wettability of NC surfaces and superhydrophobic films can be created from the hierarchical structures of NCs functionalized by dithiocarbamates with long alkyl chains. The films exhibiting tunable hydrophobic functionality also display interesting optical properties. Fig. 10 (a, b) and (c, d) show the photographs of a water drop placed on the surfaces created by CdS-D-DDAm and CdS-D-PAAm, respectively. These films both display yellow-green color under daylight. Under UV light, the film of CdS-D-DDAm shows blue emission while that of CdS-D-PAAm NCs shows light pink emission, which is consistent

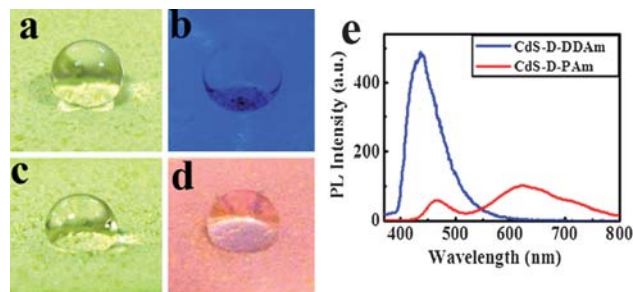


Fig. 10 Digital photographs of a water drop on the surface of (a, b) CdS-D-DDAm and (c, d) CdS-D-PAAm: (a, c) under daylight, (b, d) under irradiation with a 302 nm UV light. (e) The corresponding PL spectra of the NCs ($\lambda_{\text{ex}} = 360$ nm).

with the corresponding PL spectra (Fig. 10e). These luminescent photographs visually demonstrate the bifunctional photoluminescent-hydrophobic properties of the synthesized NCs. Therefore, the present strategy provides a new approach to technologies requiring both optical imaging and self-cleaning function.

Conclusions

This work has demonstrated a simple and facile strategy for fabricating bifunctional photoluminescent-superhydrophobic CdS NCs with controlled diverse hierarchical structures via a novel interfacial self-assembly procedure. Wire-like, belt-like, and even sheet-like microstructures can be obtained through simply varying the structures of the directing molecules. The dithiocarbamate-functionalized CdS NCs after interfacial assembly present high performance of photoluminescence compared with those of the parent CdS NCs, especially in high quantum yields. Simultaneously, the introduction of dithiocarbamate ligands derived from the reactions of carbon disulfide and amine-containing ligand with long alkyl chain can significantly enhance the hydrophobic properties of NCs in this case, which will contribute a promising way to fabricate bifunctional photoluminescent-superhydrophobic films. More broadly practical application to this approach for dithiocarbamate-functionalized NCs with advantageous functionalities may follow.

Acknowledgements

This work was financially supported by the National Natural Science Foundation of China (Grants 20606016, 10676013 NASA, 10976012 NASA), "863" Important National Science & Technology Specific Project (Grant 2007AA06A402), the National Science Foundation for Jiangsu Higher Education Institutions of China (Grant 07KJA53009), National Key Technology R&D Program in the 11th Five Year Plan of China (2006BAE03B02-1) and doctoral thesis innovation of NJUT (Grant No. BSCX200708).

References

- 1 J. H. Lim, C. K. Kang, K. K. Kim, I. K. Park, D. K. Hwang and S. J. Park, *Adv. Mater.*, 2006, **18**, 2720.
- 2 V. I. Klimov, A. A. Mikhailovsky, S. Xu, A. Malko, J. A. Hollingsworth, C. A. Leatherdale, H. J. Eisler and M. G. Bawendi, *Science*, 2000, **290**, 314.
- 3 M. Law, H. Kind, B. Messer, F. Kim and P. D. Yang, *Angew. Chem., Int. Ed.*, 2002, **41**, 2405.

- 4 H. Zhang, C. L. Wang, M. J. Li, J. H. Zhang, G. Lu and B. Yang, *Adv. Mater.*, 2005, **17**, 853.
- 5 S. Y. Yang, Q. Li, L. Chen and S. Chen, *J. Mater. Chem.*, 2008, **18**, 5599.
- 6 B. C. Das and J. Pal, *ACS Nano*, 2008, **2**, 1930.
- 7 J. M. Pietryga, D. J. Werder, D. J. Williams, J. L. Casson, R. D. Schaller, V. I. Klimov and J. A. Hollingsworth, *J. Am. Chem. Soc.*, 2008, **130**, 4879.
- 8 J. Wang, D. Y. Wang, N. S. Sobal, M. Giersig, M. Jiang and H. Möhwald, *Angew. Chem., Int. Ed.*, 2006, **45**, 7963.
- 9 Y. Lin, H. Skaff, T. Emrick, A. D. Dinsmore and T. P. Russell, *Science*, 2003, **299**, 226.
- 10 C. N. R. Rao and K. P. Kalyanikutty, *Acc. Chem. Res.*, 2008, **41**, 489.
- 11 H. Tetsuka, T. Ebina and F. Mizukami, *Adv. Mater.*, 2008, **20**, 3039.
- 12 X. J. Feng and L. Jiang, *Adv. Mater.*, 2006, **18**, 3063.
- 13 S. Chen, C. H. Hu, L. Chen and N. P. Xu, *Chem. Commun.*, 2007, 1919.
- 14 H. Y. Erbil, A. L. Demirel, Y. Avci and O. Mert, *Science*, 2003, **299**, 1377.
- 15 J. Hong, W. K. Bae, H. Lee, S. Oh, K. Char and F. Caruso, *Adv. Mater.*, 2007, **19**, 4364.
- 16 Z. Z. Gu, H. Uetsuka, K. Takahashi, R. Nakajima, H. Onishi, A. Fujishima and O. Sato, *Angew. Chem., Int. Ed.*, 2003, **42**, 894.
- 17 H. Zhang, Z. C. Cui, Y. Wang, K. Zhang, X. L. Ji, C. L. Lü, B. Yang and M. Y. Gao, *Adv. Mater.*, 2003, **15**, 777.
- 18 J. Aldana, Y. A. Wang and X. G. Peng, *J. Am. Chem. Soc.*, 2001, **123**, 8844.
- 19 L. R. Hou, L. Chen and S. Chen, *Langmuir*, 2009, **25**, 2869.
- 20 M. H. Park, Y. Ofir, B. Samanta, P. Arumugam, O. R. Miranda and V. M. Rotello, *Adv. Mater.*, 2008, **20**, 4185.
- 21 Y. Zhao, W. Pérez-Segarra, Q. C. Shi and A. Wei, *J. Am. Chem. Soc.*, 2005, **127**, 7328.
- 22 F. Dubois, B. Mahler, B. Dubertret, E. Doris and C. Mioskowski, *J. Am. Chem. Soc.*, 2007, **129**, 482.
- 23 F. E. Critchfield and J. B. Johnson, *Anal. Chem.*, 1956, **28**, 430.
- 24 H. Zhang, L. P. Wang, H. M. Xiong, L. H. Hu, B. Yang and W. Li, *Adv. Mater.*, 2003, **15**, 1712.
- 25 X. H. Zhong, M. Y. Han, Z. L. Dong, T. J. White and W. Knoll, *J. Am. Chem. Soc.*, 2003, **125**, 8589.
- 26 J. Nanda, S. Sapra, D. D. Sarma, N. Chandrasekharan and G. Hodes, *Chem. Mater.*, 2000, **12**, 1018.
- 27 Z. Tang, N. A. Kotov and M. Giersig, *Science*, 2002, **297**, 237.
- 28 Y. X. Zhang, J. Guo, T. White, T. T. Y. Tan and R. Xu, *J. Phys. Chem. C*, 2007, **111**, 7893.
- 29 N. N. Zhao, D. C. Pan, W. Nie and X. L. Ji, *J. Am. Chem. Soc.*, 2006, **128**, 10118.
- 30 B. Fritzing, W. Moreels, P. Lommens, R. Koole, Z. Hens and J. Martins, *J. Am. Chem. Soc.*, 2009, **131**, 3024.
- 31 N. Gaponik, D. V. Talapin, A. L. Rogach, A. Eychmuller and H. Weller, *Nano Lett.*, 2002, **2**, 803.
- 32 W. H. Liu, H. S. Choi, J. P. Zimmer, E. Tanaka, J. V. Frangioni and M. Bawendi, *J. Am. Chem. Soc.*, 2007, **129**, 14530.
- 33 W. M. Faustino, O. L. Malta, E. E. S. Teotonio, H. F. Brito, A. M. Simas and G. F. Sá, *J. Phys. Chem. A*, 2006, **110**, 2510.
- 34 M. H. Park, Y. Ofir, B. Samanta and V. M. Rotello, *Adv. Mater.*, 2009, **21**, 2323.
- 35 C. Liu, D. M. Shen and Q. Y. Chen, *J. Am. Chem. Soc.*, 2007, **129**, 5814.